# Near-field spatial variation in similarity spectra decomposition of a Mach 1.8 laboratory-scale jet

Aaron B. Vaughn, Tracianne B. Neilsen, Kent L. Gee, Koji Okamoto, and Masahito Akamine

Citation: Proc. Mtgs. Acoust. **29**, 045004 (2016); doi: 10.1121/2.0000456
View online: http://dx.doi.org/10.1121/2.0000456
View Table of Contents: http://asa.scitation.org/toc/pma/29/1
Published by the Acoustical Society of America

Proceedings of Meetings on Acoustics

Volume 29 http://acousticalsociety.org/

## 172nd Meeting of the Acoustical Society of America

Honolulu, Hawaii
28 November – 02 December 2016

## Physical Acoustics: Paper 2aPA9

# Near-field spatial variation in similarity spectra decomposition of a Mach 1.8 laboratory-scale jet

**Aaron B. Vaughn, Tracianne B. Neilsen, Kent L. Gee**
*Department of Physics and Astronomy, Brigham Young University, Provo, UT; a5vaughn@byu.edu, tbn@byu.edu, kentgee@byu.edu*

**Koji Okamoto, Masahito Akamine**
*Department of Advanced Energy, The University of Tokyo, Kashiwa, Chiba, Japan; k-okamoto@k.u-tokyo.ac.jp, akamine@thermo.t.u-tokyo.ac.jp*

The primary source of supersonic jet noise originates from the interaction of the turbulent flow with the ambient air. Tam et al. [AIAA Paper 96-1716 (1996)], proposed similarity spectra for a two-source model corresponding to omnidirectional fine-scale turbulence structures (FSS) and directional large-scale turbulent structures (LSS). These empirical similarity spectra agree reasonably with angular variation in mid and far-field spectra of both military and laboratory-scale jets. Near-field measurements of an ideally expanded, Mach 1.8 laboratory-scale jet from the Hypersonic and High-Enthalpy Wind Tunnel at Kashiwa Campus of the University of Tokyo were analyzed. Similarity spectra decompositions adequately describe the turbulent mixing noise as close as 10 jet diameters. Neglecting the effect of the hydrodynamic field, the LSS spectrum provides consistent fits at 15°-40° from the jet axis. A combination of LSS and FSS spectra match the measured spectra at 45°-55°. FSS spectrum matches the spectra at angles greater than 60°, except very close to the nozzle exit plane where there is an overprediction at high frequencies. Comparison of near and mid-field locations may provide insights into propagation radials.

Published by the Acoustical Society of America

 [DOI: 10.1121/2.0000456]

## 1. INTRODUCTION

The primary noise sources from a supersonic jet are produced by the interaction of the turbulent flow with the ambient air. This turbulent mixing noise is responsible for the directivity of the jet noise. One model for the turbulent mixing noise, proposed by Tam *et al.*[1,2] postulates that turbulent structures with different length scales produce different types of sound. The large-scale turbulent structures generate partially correlated, directional noise, and are responsible for the dominant radiation lobe (shown with a black arrow in Figure 1a). The fine-scale turbulent structures act independently and produce omnidirectional radiation, which can be detected outside the dominant lobe as illustrated in Figure 1a. Tam *et al.*[1] examined a large database of far-field spectra from laboratory-scale jets that had been scaled to a distance of $100D_j$, where $D_j$ is the jet nozzle exit diameter, and found empirical fits for the spectral shapes of the two types of turbulent mixing noise. These two similarity spectra have subsequently been shown to match far-field spectra for turbulent mixing noise of lab-scale jets[1,2,3] and mid-field spectra of tactical aircraft.[4,5,6] The direction of the dominant radiation lobe and thus the regions in which the two similarity spectra agree with measured spectra depends on both the speed and temperature of the jet.[7,8,9] This paper examines if the similarity spectra apply in the near field of a laboratory-scale jet.

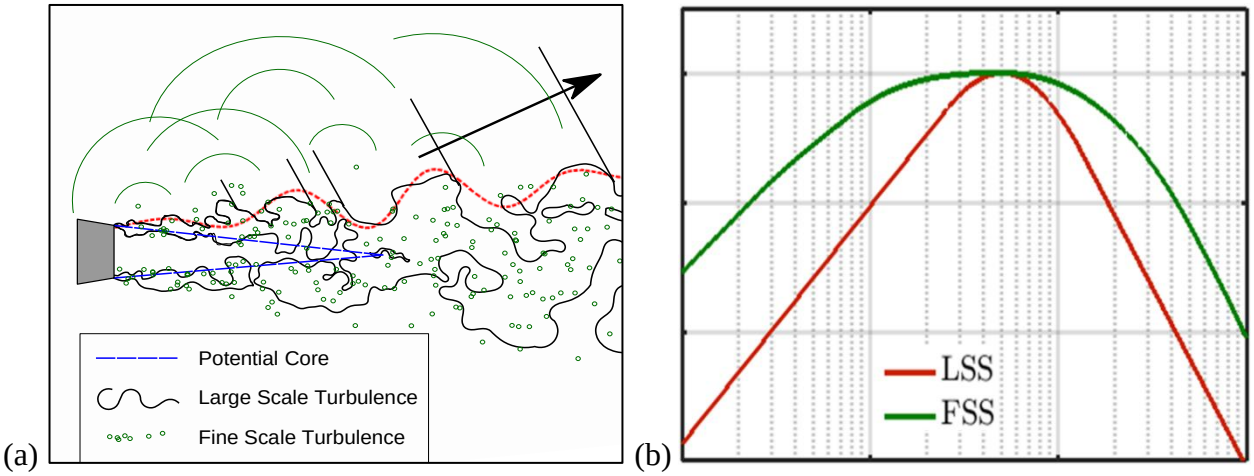


***Figure 1. (a) Similar to Figure 4 in Ref. [2]. (b) Similarity spectral shapes.***

The empirical similarity spectra associated with the two kinds of turbulent mixing noise, illustrated in Figure 1b, have different shapes. The similarity spectrum associated with the large-scale structures (LSS) has a more peaked shape, with a steeper spectral slope above and below the peak frequency than the fine-scale similarity spectrum (FSS), which has a broader spectral peak.[1] With the spectral shape fixed, amplitude and peak frequencies of the FSS and/or LSS spectra can be adjusted to investigate if these spectral shapes are a good representation of measured spectra. According to the literature,[1,3,6] the LSS spectrum is expected to yield a good match at the farthest aft locations, a mixed region, where contributions from both similarity spectra are detected, is expected around 45°-70° from the jet axis, and FSS spectrum is expected to dominate at angles greater than 90° from the jet axis.

As similarity spectra were developed from far-field measurements, this paper focuses on the applicability of the similarity spectra to measurements taken in the mid and near field of a supersonic, ideally expanded jet. The experimental setup is described and the process of matching the similarity spectra to the measurements is explained. Examples of how the similarity spectra agree are given and limitations are discussed. To provide evidence for the validity of the similarity spectra fits at these near and mid-field locations, the overall sound pressure level of the measured

data are compared to similarity spectra levels. In addition, spatial distribution in the similarity spectra decompositions is evaluated to obtain insights about possibly sound propagation radials.

## 2. EXPERIMENT

Acoustical measurements of an unheated, Mach 1.8 laboratory-scale jet were collected at the Hypersonic and High-Enthalpy Wind Tunnel at the Kashiwa Campus of the University of Tokyo.[10] The 20 mm diameter ($D_j$), converging-diverging nozzle was ideally expanded at Mach 1.8. Due to the non-anechoic environment, reflecting surfaces were wrapped in fiberglass as seen in Figure 2b. Using National Instruments PXI-4498 cards sampling at 204.8 kHz, calibrated pressure waveform data were simultaneously acquired at 40 channels. During each jet blow, which lasted between 60-90 seconds, data were acquired for 6.1 seconds at each location, then the automated positioning system moved the line array of 16 microphones to scan the near field. The ambient pressure, temperature, and humidity of the jet facility were recorded for each test using a Kestrel 4500B weather station.

(a)

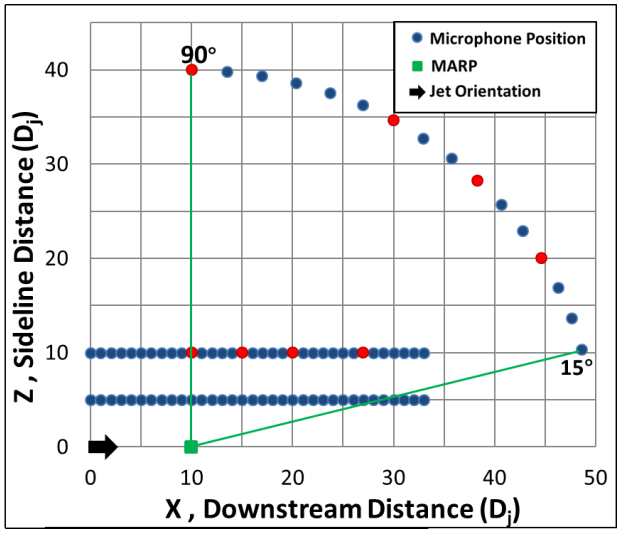


(b)

***Figure 2. (a) Schematic of the measurement locations. Red dots indicate locations examined in Figures 5 and 6. (b) Fiberglass and jet nozzle.***

This analysis focuses on data collected from microphones on a mid-field arc and near-field line arrays, as illustrated in Figure 2a. The arc, shown in Figure 3a, contained 6.35 mm (1/4") G.R.A.S. 40BE Type 1, free-field microphones. Each arc microphone was $40D_j$ radial distance from the measurement array reference point (MARP) located $10D_j$ downstream of the jet nozzle exit plane. The angular positions of the 16 arc microphones were defined relative to the MARP and spanned 15°-90° with 5° spacing. The arc's free-field microphones were pointed at the MARP providing a flat bandwidth up to ~100 kHz. The line arrays were parallel to the jet centerline but vertically displaced at $5D_j$ and $10D_j$ (Figure 3b). The line arrays contained 6.35 mm (1/4") G.R.A.S. 46BG Type 1, pressure microphones. The metal rake, visible in Figure 3b, held 16 microphones with $1D_j$ spacing and was moved by an automatic positioning system to cover the locations shown in Figure 2a. Measurements were taken at $5D_j$ and $10D_j$ (above the jet centerline) such that the microphone locations spanned x = 0-$33D_j$. The line array microphones were oriented perpendicular to the jet centerline, such that most of the sound was incident at grazing angle providing relatively flat frequency response up to 70 kHz. Microphone gridcaps were removed for all measurements.

(a) 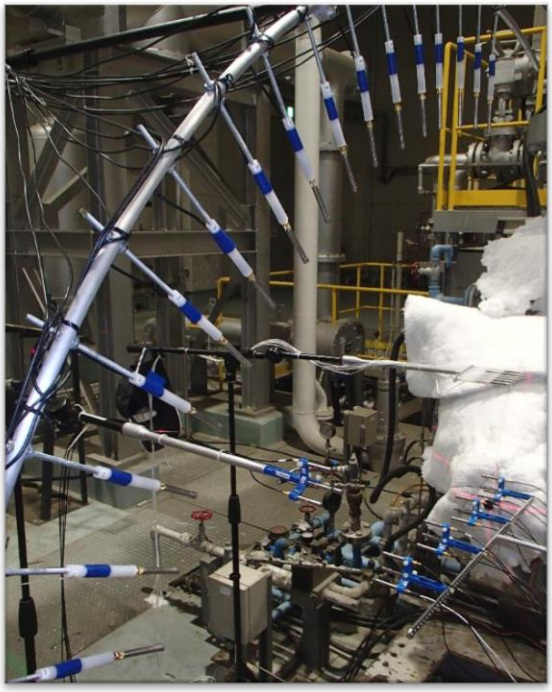 (b) 

***Figure 3. (a) Microphone arc array. (b) Microphone line array.***

To investigate the effects of the nearness of the $5D_j$ and $10D_j$ line arrays to the jet flow, the power spectral density (PSD) is examined at various downstream distances (see Figure 4). In the far field, the noise from an ideally expanded, supersonic jet consists of turbulent mixing noise. Close to the flow, however, the noise also contains hydrodynamic or near field noise, which decays evanescently with distance. As the line arrays are parallel to the jet centerline and the shear layer of the jet is expanding, the microphones at larger x, in Figure 2a, are closer to the flow. The presence of the hydrodynamic field[11,12,13] causes a boost in the low-frequency content of the spectrum as can be seen at z = $20D_j$ and $30D_j$ on the $5D_j$ line array (Figure 4a) and at z = $30D_j$ on the $10D_j$ line array (Figure 4b). As the hydrodynamic field is not present in the far-field measurements used to develop the similarity spectra, its effect is disregarded when fitting the similarity spectra to near-field data.

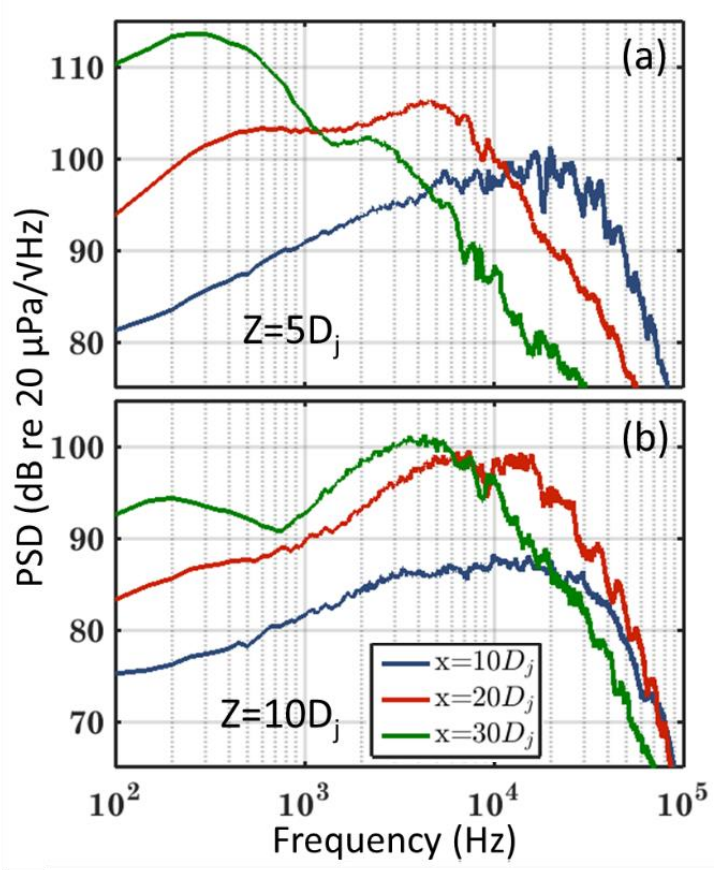


***Figure 4. PSD of the $5D_j$ (a) and $10D_j$ (b) line array at varying downstream distances.***

## 3. SIMILARITY SPECTRA ANALYSIS

The spectral content of noise measured near the ideally expanded Mach 1.8 jet in the near and mid fields are compared to the similarity spectra proposed by Tam *et al.* to see if they capture the spectral shape of the mixing noise in the near field. The similarity spectra matching process has some latitude but is guided by the following principles. Due to the microphone bandwidth and the presence of the hydrodynamic field, a frequency range from 500 Hz to 70 kHz, which corresponds to a Strouhal number of 0.02 to 2.7, is primarily used to fit the similarity spectra. When matching the similarity spectra to measured spectra, as previously described, the peak frequency and peak level of the similarity spectra are adjusted until a suitable match is found. In some cases, both the FSS and LSS spectra are needed to fit the measured spectra. The resulting mix of the two spectra is then considered the total similarity spectrum. Examples of the similarity spectra matches are shown for the locations indicated by red dots in Figure 2.

Comparisons between the similarity spectra and measured spectra for the near-field $10D_j$ line array reveal that, in most cases, the similarity spectra accurately describe the near-field turbulent mixing noise. To illustrate the spatial variation, similarity spectra fits are shown in Figure 5 for the locations shown as red dots of the $10D_j$ line array in Figure 2. Starting from the location above the MARP, $x = 10D_j$ (Figure 5a), the FSS spectrum is sufficient to match the spectrum of the jet noise. The only discrepancy is that there is a high frequency roll off at 30 kHz in the data. At the next location downstream, $x = 15D_j$, (Figure 5b) again the FSS spectrum provides a strong fit until 30

kHz where the measured spectrum rolls off steeper than the FSS spectrum predicts. This is curious because it is below the microphone roll-off frequency and is not seen when the same microphone is placed at locations further downstream. At $20D_j$ downstream (Figure 5c), a mix of the FSS and LSS spectra are needed to catch the broadness of the spectral shape above and below the peak frequency and to capture the width of the peaked region. Some jaggedness in the measured spectrum due to reflections exist; nevertheless, the combination of FSS and LSS spectra matches the overall spectral shape. At the last location, x = $27D_j$ , (Figure 5d) only the LSS spectrum is needed to match the measured spectrum. It appears that the similarity spectra adequately describes the turbulent mixing noise at $10D_j$ from the jet centerline, except close to the nozzle exit plane where the FSS spectrum overpredicts the measured spectra.

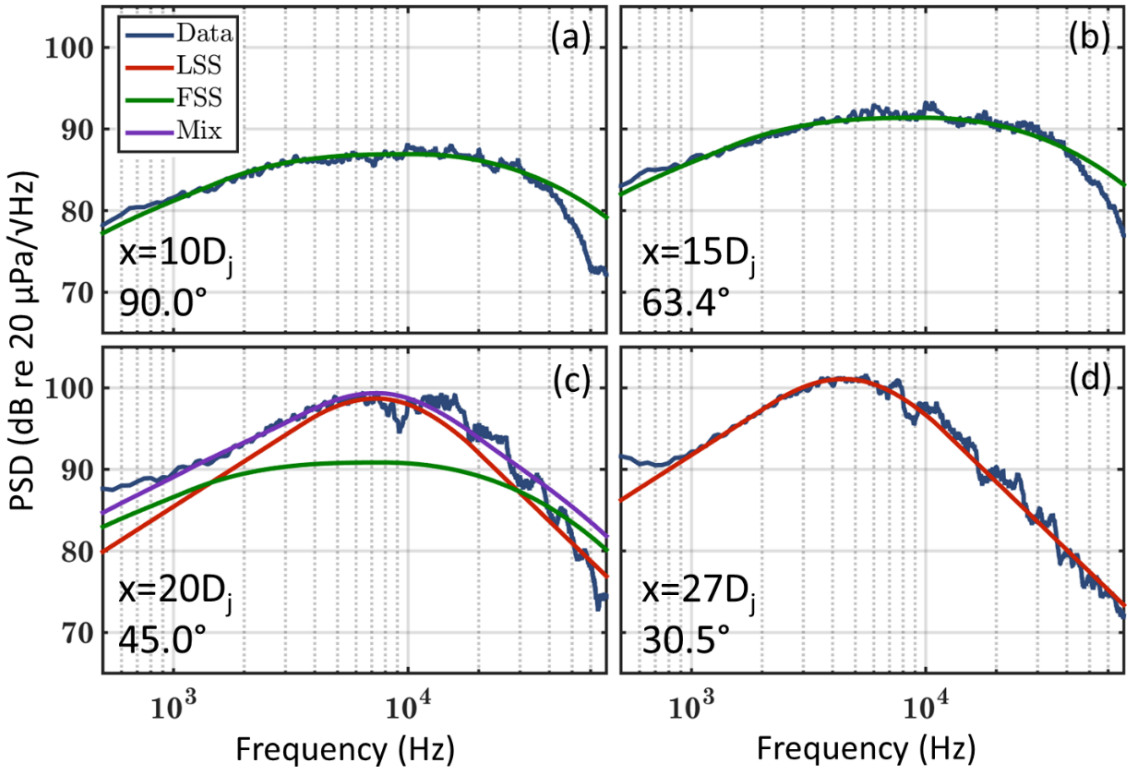


***Figure 5. Comparison of similarity spectra with the measured spectra (blue) at (a) x = $10D_j$, 90°, (b) x = $15D_j$, 60°, (c) x = $20D_j$, 45°, and (d) x = $27D_j$, 30° on the $10D_j$ line array.***

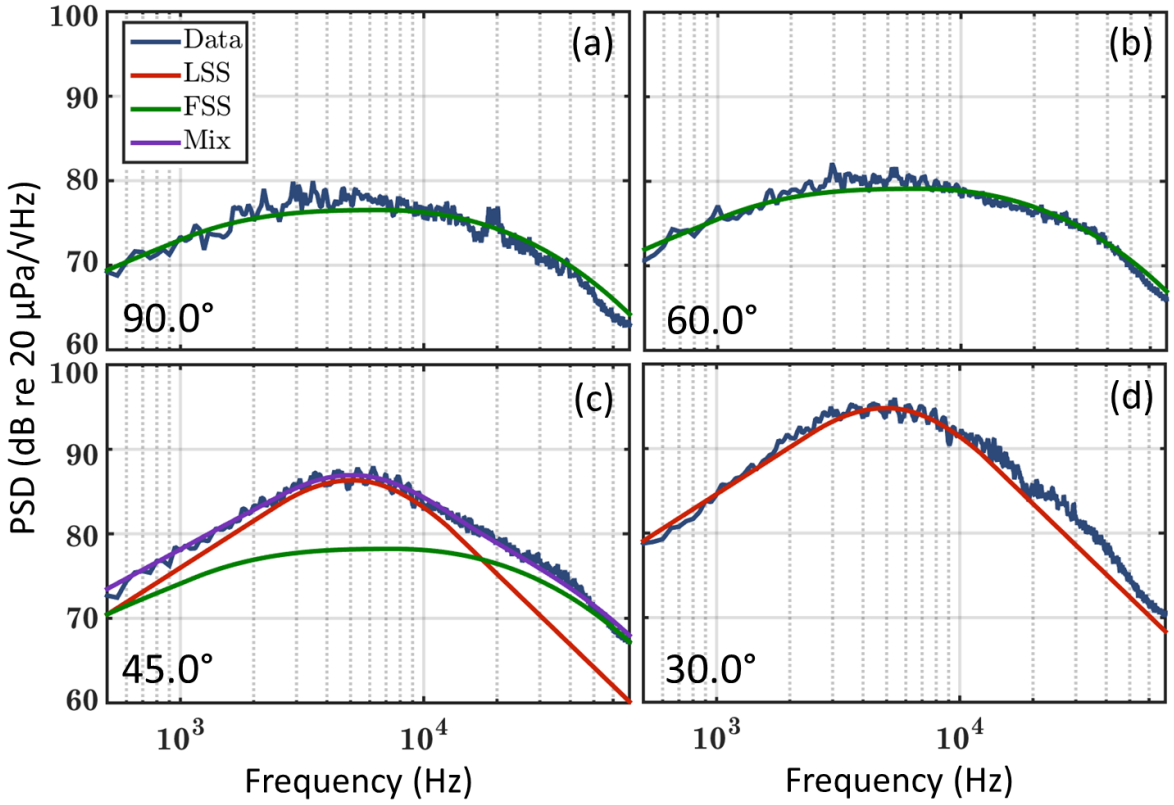


***Figure 6. Comparison of similarity spectra with the measured spectra (blue) at (a) θ = 90°, (b) θ = 60°, (c) θ = 45°, and (d) θ = 30° on the $40D_j$ arc.***

The agreement between similarity spectra and measured spectra along the $40D_j$ arc show many of the same features. The similarity spectra fits are displayed in Figure 6 for locations shown as red dots in Figure 2. These locations are selected because they have approximately same angle, θ, as those shown in Figure 5 for the $10D_j$ line array. The plots in Figure 6a and 6b show the measured spectra at θ = 90° and 60° can be fit with only FSS spectrum across the entire frequency range, unlike the $10D_j$ line array, the measured spectra at $40D_j$ do not have a steep roll off at 30 kHz. At θ = 45° (Figure 6c), a mix between the two similarity spectra produces an excellent fit both above and below the peak region. Figure 6d plot shows that at θ = 30° good agreement is obtained with only the LSS spectrum, with a slight discrepancy in the data between 20 and 50 kHz, possibly due to the non-anechoic measurement environment. In contrast to the $10D_j$ line array, there is no steep roll off at 30 kHz in the data. The angular regions over which the FSS and LSS similarity spectra adequately represent the measured spectra in Figures 5 and 6 compare agreeably with those expected by the literature.[1,2,3]

Another way to evaluate the appropriateness of the similarity spectra fits is to quantify how well the similarity spectra decompositions represent spatial variation in the overall sound pressure level (OASPL). The level associations with the FSS and LSS spectral fits are shown along with the measured levels in Figure 7. Across the $40D_j$ arc (Figure 7a), there is good agreement between the similarity spectra levels and the measured levels in the region dominated by the FSS spectrum with a smoothly varying transition to a region of solely LSS spectrum. At angles closest to the jet centerline, θ = 15°-40°, the LSS-based levels are about 1 dB lower than the measured level. For comparison, the OASPL along the $10D_j$ line array also shows a smoothly varying trend from FSS

to LSS as x increases. For x > $5D_j$, the similarity spectra levels match the OASPL. For x < $5D_j$, however, the similarity spectra levels overpredict OASPL because of the lack of high-frequency energy (shown in Figure 5a and 5b) Despite the discrepancy of about 2-3 dB in the forward direction in the near field, the similarity spectra decompositions provide a good representation of the overall levels in the near and mid fields.

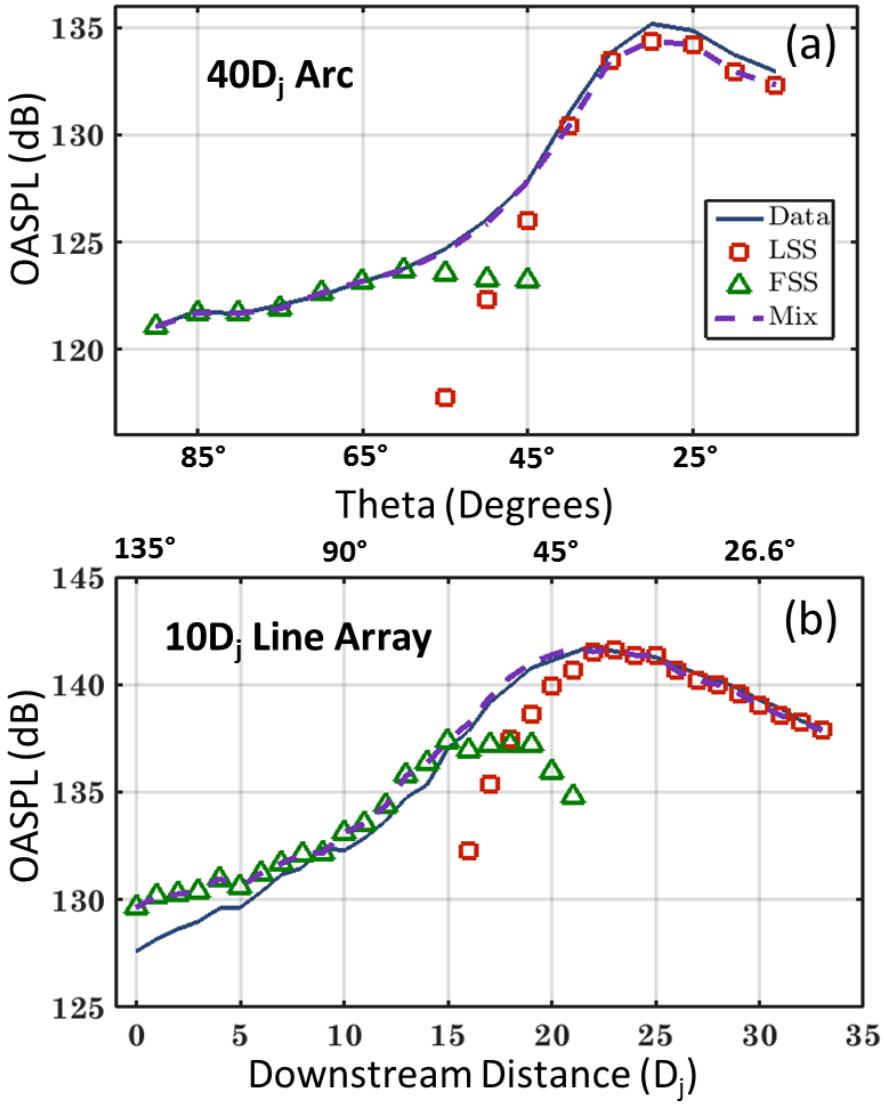


***Figure 7. OASPL of the data and similarity spectra decompositions along (a) the 40$D_j$ arc and (b) the 10$D_j$ line array.***

The similarity spectra decompositions were completed for all locations shown in Figure 2. Color-coding each microphone location according to the type of similarity spectra fit (LSS, FSS, or mix) can potentially yield insights into propagation radials (Figure 8). Using the MARP at 10$D_j$ as the origin, the plot in Figure 8a shows a consistent trend along radials. Starting from the MARP and moving out along the 90° radial, FSS spectrum provides a good fit at both line arrays and the arc. Moving along the 45° radial, each location requires a combination of FSS and LSS to match the measured spectrum. The 30° radial consistently needs only the LSS spectrum. To examine whether this choice of the MARP at 10$D_j$ dictates the constancy of similarity spectral decomposition along radials, comparisons are made with other possible choices for the MARP.

When the MARP is moved to $5D_j$ (Figure 8b), the propagation radials are no longer consistent. The fourth line down from the top, for example, starts in an LSS region, but progresses to a mix region at the $10D_j$ line array and arc. Similarly, the second radial from the bottom on the $5D_j$ MARP plot starts in a mix region and progresses to an LSS dominated region. Moving the MARP the other direction to $15D_j$ (Figure 8c) also yields inconsistencies as the first three radials from the top all begin in a mix region and progress to an FSS dominated region as distance from the MARP increases. The choice of $10D_j$ for the MARP is consistent with the similarity spectra decompositions for this ideally expanded, Mach 1.8 jet.

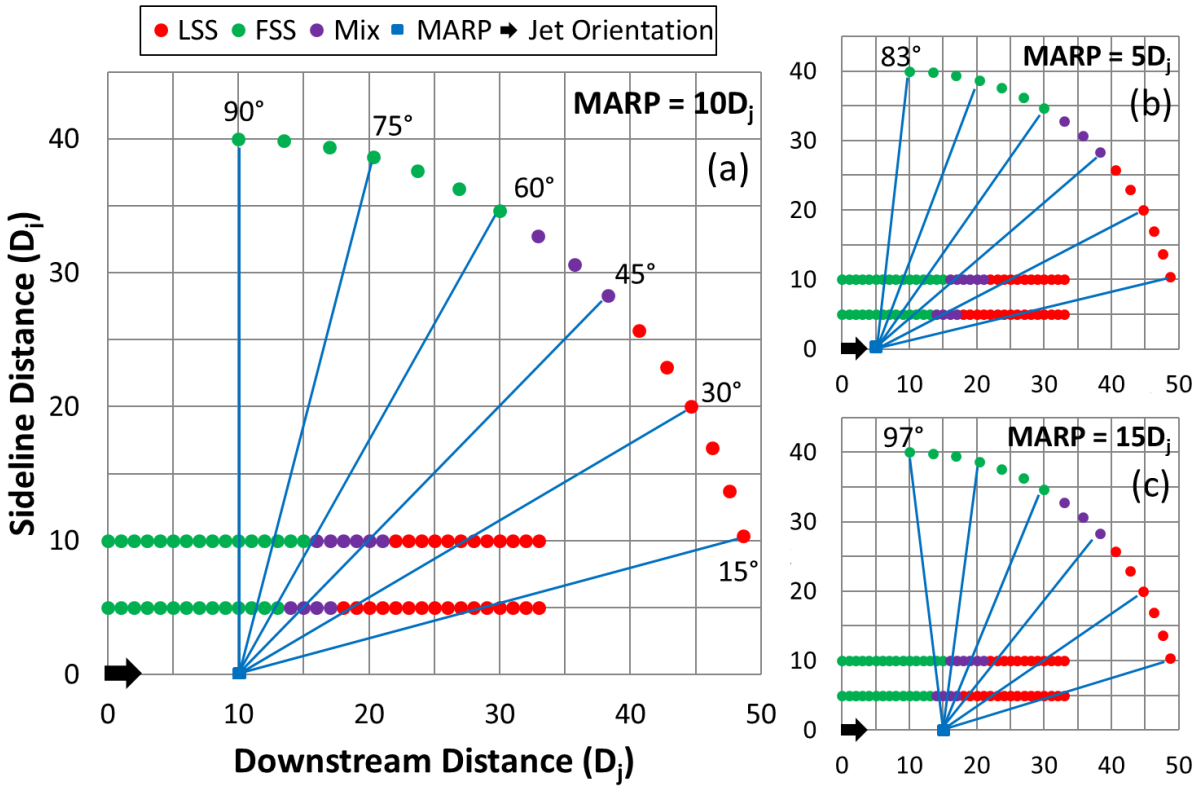


***Figure 8. Color-coding of the similarity spectra decompositions at the measurement locations with radials from a MARP of $10D_j$ (a), $5D_j$ (b) and $15D_j$ (c). Green dots indicate that the FSS spectrum matches the spectra at that location; red dots mean that solely LSS spectrum is needed, and purple dots are at locations where both FSS and LSS spectra are required.***

## 4. CONCLUSION

Even though the empirical similarity spectra for turbulent mixing noise were developed by Tam *et al.*[1] using far-field jet noise, the fine and large-scale similarity spectra have been shown to match the spectral shapes of the jet noise in the mid field ($40D_j$) of a Mach 1.8 jet and in the near field ($5\text{-}10D_j$) with a few caveats. First, care must be taken when fitting the similarity spectra in the near field that contributions from the hydrodynamic field are not considered in matching the spectra. Second, in the near field of the jet very close to the nozzle exit plane, the FSS spectrum overpredicts the high frequency content, as the spectra measured in this region show a sharp roll off at high frequencies. It is unlikely that this is microphone effect as it is observed over a spatial aperture of more than $10D_j$ and the same microphones do not exhibit this roll off when placed farther downstream. The agreement between the similarity spectra developed from far-field jet

noise databases to noise in the near and mid field is quite remarkable and is a sign of their ability to generally describe the features of turbulent mixing noise. The spatial aperture of this study provided the opportunity to analyze if the similarity spectra decomposition may assist in determining propagation radials: the choice of MARP = $10D_j$ provided a consistent similarity spectra decomposition along radials for this unheated, Mach 1.8 jet.

## ACKNOWLEDGMENTS

The acoustical measurements at the Hypersonic and High-Enthalpy Wind Tunnel at the Kashiwa Campus of the University of Tokyo were made possible by an Invitation Fellowship for Research in Japan.

## REFERENCES

[1] C. K. W. Tam, M. Golebiowski and J. M. Seiner, "On the two components of turbulent mixing noise from supersonic jets," AIAA Paper 96-1716, (1996).

[2] C. K. W. Tam, K. Viswanathan, K. K. Ahuja and J. Panda, "The sources of jet noise: Experimental evidence," J. Fluid Mech. **615**, 253–292 (2008).

[3] C. K. W. Tam, N. N. Pastouchenko and R. H. Schlinker, "Noise source distribution in supersonic jets," J. Sound Vibration **291**, 192-201, (2006).

[4] T. B. Neilsen and K. L. Gee, "Spectral characterization in the near and mid-field of military jet aircraft noise," AIAA paper 2013-2191 (2013).

[5] T. B. Neilsen, K. L. Gee, A.T. Wall, M. M. James and A. A. Atchley, "Comparison of supersonic full-scale and laboratory-scale jet data and the similarity spectra for turbulent mixing noise," Proc. Meet. Acoust. **19**, 040071 (2013).

[6] T. B. Neilsen, K. L. Gee, and A. T. Wall, "Similarity spectra analysis of high-performance jet aircraft noise," J. Acoust. Soc. Am. **133**, 2116-2125 (2013).

[7] K. Viswanathan, "Aeroacoustics of hot jets," J. Fluid Mech. **516**, 39-82 (2004).

[8] K. Viswanathan and M. J. Czech, "Role of jet temperature in correlating jet noise," AIAA J. **47**, 1090–1106 (2009).

[9] J. Laufer, R. Schlinker, and R. E. Kaplan, "Experiments on supersonic jet noise," AIAA J. **14**, 489-498 (1976).

[10] Masahito Akamine, Yuta Nakanishi, Koji Okamoto, Susumu Teramoto, Takeo Okunuki, and Seiji Tsutsumi. "Acoustic phenomena from correctly expanded supersonic jet impinging on inclined plate," AIAA J. **53**, 2061-2067 (2015).

[11] K. L. Gee, T. B. Neilsen, E. B. Whiting, D. K. Torrie, M. Akamine, K. Okamoto, and S. Tsutsumi, "Application of a phase and amplitude gradient estimator to intensity-based laboratory-scale jet noise source characterization," *Sixth Berlin Beamforming Conference,* BeBeC-2016-D3, (Berlin, Germany, February 2016).

[12] H.E. Hafsteinsson, L.-E. Eriksson, N. Andersson, D.R. Cuppoletti, E. Gutmark, E. Prisell, "Near-field and far-field spectral analyzis of supersonic jet with and without fluidic injection," AIAA paper 2014-1403 (2014)

[13] T. Suzuki and T. Colonius, "Instability waves in a subsonic round jet detected using a near-field phased microphone array," J. Fluid Mech. **565**, 197-226 (2006)